The Effect of Acute Hypoxia and Hyperoxia on the Slow Multifocal Electroretinogram in Healthy Subjects

Kristian Klemp, Henrik Lund-Andersen, Birgit Sander, and Michael Larsen

PURPOSE. To characterize the topographic response of the healthy human retina to acute oxygenation changes in vivo, using multifocal electroretinography (mfERG).

METHODS. Ten eyes in 10 subjects were examined while they breathed 21% oxygen (normoxia), 10% oxygen (hypoxia, with 90% nitrogen), or 100% oxygen (hyperoxia). Capillary oxygenation was monitored by percutaneous infrared oximetry.

RESULTS. Compared with normoxia (mean Pao_2, 124 mm Hg), hypoxia (mean Pao_2, 36 mm Hg) was associated with an overall mfERG amplitude reduction, including a reduction in the multifocal oscillatory potentials (mfOPs). The hypoxic amplitude reduction of the first-order P1 response decreased monotonically ($P < 0.0001$) from 38.5% at 0° to 2° eccentricity to 17.8% at the highest eccentricity (25°). Likewise, the amplitude reduction of first-order N2 decreased from 33.0% centrally to 18.3% at the highest eccentricity ($P = 0.0019$). In contrast, hypoxia only reduced the average first-order N1 amplitude by 9.5% ($P = 0.016$). Hypoxia also reduced mfOP amplitudes, by 16.6% to 34.8%, but no effect of eccentricity was detectable. Hyperoxia had no significant effect on amplitude. Neither hypoxia nor hyperoxia had any effect on the latency of the P1 implicit times.

CONCLUSIONS. The present study demonstrated regional differences in response to hypoxia. The origin of this difference is not known but may be explained by a combination of differences in cone structure, circulation of different regions, or differences in the microenvironment around different cones. The function of the central retina is expected to be more susceptible to the hypoxia that may occur in disease. The relative effect of hypoxia on the photopic N1 and P1 is similar to that on the scotopic a- and b-wave in other mammals, and the present work extends the current knowledge by showing regional effects that were previously undetected. (*Invest Ophthalmol Vis Sci.* 2007;48: 3405–3412) DOI:10.1167/iovs.06-0471

The anatomy of the human retina gives priority to high transparency and photoreceptor density. The retinal blood supply and oxygenation are sparse compared with the rate of oxygen consumption, which is higher per unit weight than in other parts of the brain.[1,2] Phototransduction and neural signaling are energy-demanding processes that appear to have been developed in response to an evolutionary pressure for high-performance vision. To produce the necessary energy under the constraints of a limited blood supply, the retina utilizes its oxygen supply completely, with the tension reaching a minimum of less than 5 mm Hg in the outer retina in the dark-adapted state,[3–5] and then supplements its requirements by extensive use of anaerobic glycolysis, which extracts only a fraction of the energy available in glucose. The performance of the retina is limited by the supply of oxygen,[6] but the dependence on oxygen is likely to vary by layer, eccentricity, and cell type, cell density, and the state of light adaptation.

Changes in retinal oxygen supply are believed to be an important factor in diabetic retinopathy,[7] in which the distribution of disease varies greatly with eccentricity. Understanding acute changes and their variation with eccentricity resulting from reduced and increased oxygen supply to the normal retina may aid in the discovery of mechanisms involved in the development and progression of diabetic retinopathy. In no previous study, however, has the retinal sensitivity to hypoxia and hyperoxia been examined in relation to retinal topography.

The present study was designed to assess the response of the retina in healthy subjects to acute changes in oxygen supply, using multifocal electroretinography (mfERG).

METHODS

We examined 10 eyes in 10 healthy subjects. Ophthalmic examination included determination of visual acuity, slit-lamp biomicroscopy, ophthalmoscopy, and mfERG. All participants had best visual acuities of 20/20 or better and no detectable ophthalmic disorder or chronic disease (Table 1). All subjects had arterial blood pressure lower than 140/90. Written informed consent was obtained from the participants after explanation of the nature and possible consequences of the study. The study was approved by the medical ethics committee of Copenhagen County and adhered to the tenets of the Declaration of Helsinki.

The participants were randomly assigned to have either the left or right eye tested. Pupils were dilated to a diameter of ≥7 mm with 10% phenylephrine hydrochloride and 1% tropicamide. After topical anesthesia with 0.4% oxybuprocaine hydrochloride, a Burian-Allen bipolar contact lens electrode with two built-in infrared light sources for fundus illumination (Veris IR Illuminating Electrode; EDI Inc., San Mateo, CA) was placed on the test eye using carboxymethylcellulose 1% contact fluid. The contralateral eye was occluded. A ground electrode was attached to the forehead after skin cleaning using an abrasive gel (Nuprep; D.O. Weaver & Co., Aurora, CO).

An array of stimuli was displayed on a 1.5-in. stimulator-fundus camera (Veris; EDI Inc.), which permitted optimal refraction without changing the size of the visual image and ensured fixation by real-time infrared viewing of the fundus. To facilitate fixation monitoring, the stimulus array was overlaid on the fundus monitor.

The stimulus array (Fig. 1) contained 61 hexagons scaled by eccentricity (scaling factor 12.857) displayed at a frame rate of 75 Hz. Each stimulus was modulated by using a binary m-sequence over four video frames. During the first video frame, each hexagonal stimulus was either flashed at a luminance of 200 cd/m^2 or remained dark, as did the subsequent three frames. This resulted in a minimum interval of 53.3 ms between each flash in a given hexagonal stimulus field to enhance

TABLE 1. Clinical Characteristics of Subjects

	Normoxia	Hypoxia	Hyperoxia
Age, y, mean (SD)	31.1 (2.8)		
Sex, male/female	3/7		
Saturation (%), mean (SD)	98.8 (0.8)	69.4 (2.8)	100 (0)
Heart rate (bpm), mean (SD)	63.8 (9.1)	87.5 (9.0)	60.8 (7.1)
Blood glucose (mmol/l), mean (SD)	4.8 (0.5)	4.7 (0.4)	4.9 (0.6)
Systolic blood pressure, mm Hg, mean (SD)	113.2 (10.1)		
Diastolic blood pressure, mm Hg, mean (SD)	68.8 (10.1)		

$n = 10$.

oscillatory potentials (OPs).[8] The m-sequence exponent of 13 resulted in a total recording time of 3.38 minutes, which were divided into eight short segments for patient comfort. Responses were band-pass filtered outside 10 to 300 Hz, amplified at a gain of 100,000 and sampled every 0.833 ms. Observation of loss of fixation or artifacts led to rejection of the affected recording segment and immediate rerecording. The luminance of the white stimulus was 200 and 2 cd · m^{-2} or less for the black stimulus. The surround luminance was set to 50% of the mean test field luminance (i.e., 100 cd · m^{-2}). Ambient room light was maintained throughout the study. Stimulus luminance was calibrated using the auto calibrator (EDI, Inc.) and the stimulus grid was calibrated using a grid calibrator (VERIS; EDI Inc.). Two iterations of artifact rejection were applied to the raw data and no spatial smoothing was performed. The first- and second-order (first slice) kernels were derived and implicit times and amplitudes of N1 (first negative component), P1 (first positive component), and N2 (second negative component) were measured. Mathematically, the first-order kernel is obtained by adding all the records that follow the presentation of a white hexagon (flash) and subtracting all the records that follow a black hexagon (no flash). The response elicited by the specific hexagon continuously builds up during the stimulation sequence. The second-order kernel is obtained by adding all the records after a change from white-to-black or black-to-white and subtracting all records after no change. The first slice of the second-order kernel measures the effect of an immediately preceding flash and is a measure of how the mfERG response is influenced by the adaptation to successive flashes.[9] The N1 response amplitude was measured from the starting baseline to the base of the N1 trough, the P1 response amplitude was measured from the N1 trough to the P1 peak, and the N2 response amplitude was measured from the P1 peak to the N2 trough (Fig. 2). The raw data were band-pass filtered (100–300 Hz; Veris 5.0 system), to extract the implicit times and amplitudes of the local oscillatory potentials. mfERG responses were averaged from five concentric rings and nine regions specified by coordinates relative to the fovea (Fig. 1). mfOP responses were averaged in a similar manner, except that rings 1 and 2 were averaged to improve the signal-to-noise ratio, resulting in four concentric rings and nine regions.

The study was designed as an open-label, randomized cross-over study, including a hypoxic, a hyperoxic, and a normoxic period. In each patient, three multifocal ERGs were recorded on the same day, one during hypoxia, one during hyperoxia, and one while the patient breathed atmospheric air. After stable saturation had been obtained (3–6 minutes), an uninterrupted period of 5 minutes was allowed before the first mfERG was recorded. Participants continued to breathe the same gas mixture during the recording. The mean total duration of hypoxia was 11.3 minutes. The subjects were randomized to start with the hypoxic period followed by the hyperoxic period or vice versa. They breathed a gas mixture of 10% oxygen and 90% nitrogen to induce hypoxia and 100% oxygen to induce hyperoxia.

Blood oxygenation was determined by using a NPB-40 finger pulse oximeter (Nellcor Puritan Bennet, Inc., Pleasanton, CA). The blood glucose level during a given mfERG recording period was defined as the mean of one blood glucose value recorded immediately before and one recorded immediately after the mfERG recording. Plasma glucose concentrations were determined with a blood glucose meter (Lifescan One Touch; Johnson & Johnson Co., Jacksonville, FL).

Statistical analysis of the mfERG response was made, allowing for interdependence between adjacent subfields (Fig. 1).[10] Mixed-model analysis (SAS Systems, ver. 8.2; SAS Institute, Cary, NC) returns probabilities for the effect of region or ring, together with an estimate of the difference between normal conditions and hypoxia/hyperoxia in implicit times and amplitudes. The difference in amplitude between normoxia and hypoxia was calculated as amplitude$_{normoxia}$ − amplitude$_{hypoxia}$, and for hyperoxia as amplitude$_{hyperoxia}$ − amplitude$_{normoxia}$. The same computation was used for the implicit time difference.

RESULTS

Blood Oxygen Saturation

Mean capillary saturation was 98.8% ± 0.8% (Pao$_2$ 124 ± 1.3 mm Hg)[11] during atmospheric air breathing and decreased to 69.4% ± 2.8% (Pao$_2$ 36 ± 4.1 mm Hg) while breathing 10% O$_2$
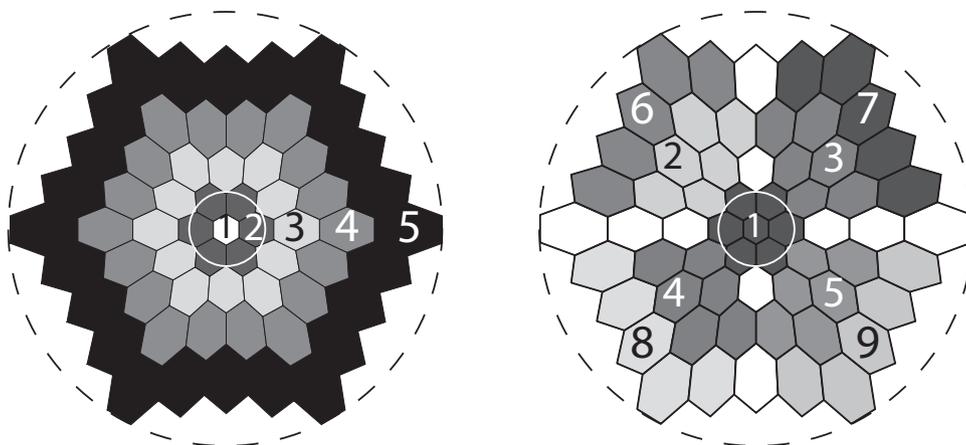

FIGURE 1. Subfield definitions applied in mfERG data analysis by five levels of eccentricity (*left*): ring 1, fovea (0°–1.4°); ring 2, parafovea (1.4°–5.6°); rings 3 (5.6°–10.8°) and 4, midmacula (10.8°–17°); and ring 5, peripheral macula (17°–25°) and by quadrants at three levels of eccentricity (*right*). Superimposed on the array of 61 hexagonal stimulus fields are *white circles* at 5° and *dashed circles* at 30°. For better signal-to-noise ratio, rings 1 and 2 of mfOP data were averaged, resulting in only four levels of eccentricity.
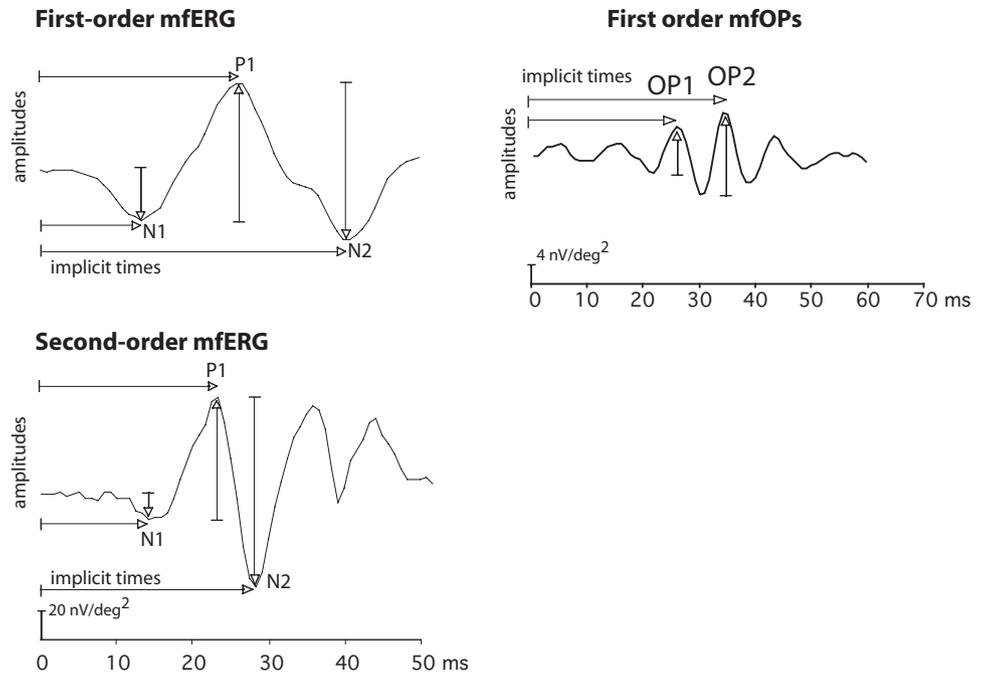
First-order mfERG

First order mfOPs

Second-order mfERG

FIGURE 2. First- and second-order mfERG waveforms and first-order mfOP waveforms averaged from all 61 hexagons with *arrows* indicating how amplitudes (*vertical*) and implicit times (*horizontal*) of the major components (N1, P1, N2, OP1 and OP2) were measured.

in 90% N_2, whereas mean capillary saturation increased to 100% ± 0.0% during the inhalation of 100% oxygen.

Hypoxia-Induced Changes in the mfERG

Hypoxia induced marked changes in mfERG amplitudes (Fig. 3), including the amplitudes of the oscillatory potentials (Fig. 4), whereas only discrete changes were observed in mfERG implicit times.

Mean P1 amplitudes were significantly reduced during hypoxia compared with normoxia (Fig. 5). This observation was consistent throughout the stimulated field, when tested by eccentricity (five concentric rings; Table 2) and by direction (nine meridional subfields, two per quadrant and a central subfield). Mean P1 amplitudes decreased during hypoxia, from 38.4% (95% CI 36.8–67.2, $P < 0.0001$) at 0° to 1.4° eccentricity (ring 1, fovea), the reduction decreasing with increasing eccentricity ($P < 0.0001$) to a low of 17.1% ($P < 0.0001$) at 25° eccentricity (Table 2, Fig. 4). No variation by quadrant was detectable. The summed response of all 61 hexagons decreased by 27.2% (19.8 nV/deg², 95% CI 14.6–24.9, $P < 0.0001$).

Hypoxia significantly reduced the mean N2 amplitude at all eccentricities (Fig. 6), most prominently in the central field, where 33% reduction was observed (from 132.72 to 88.87 nV/deg², $P = 0.0019$) and decreasing monotonically with increasing eccentricity to a low of 18.3% ($P < 0.01$) at 25° eccentricity.

N1 amplitudes were also reduced during hypoxia, but to a lesser extent than the P1 and N2 amplitudes (Fig. 7). The average N1 response decreased by 9.5% ($P = 0.016$). A U-shaped relation with eccentricity was noted, in that the N1 amplitude decreased by 12.9% ($P > 0.05$) within 0° to 2° of eccentricity, was unchanged for rings 2 and 3 (nominal amplitude change, −1.6%, $P > 0.05$), and decreased by 19.7% for ring 4 ($P = 0.004$) and by 17.3% for ring 5 ($P = 0.036$).

N1 and P1 implicit times were not detectably altered by hypoxia, whereas mean N2 implicit time averaged from the entire field (61 hexagons) was delayed by 2.06 ms (95% CI 1.3–2.8; $P < 0.0001$).

The second-order N2 amplitudes were also reduced by hypoxia, although to a lesser extent than the first-order re-

21 % Oxygen

Retinal view

Nasal   Temporal

10% Oxygen

Retinal view

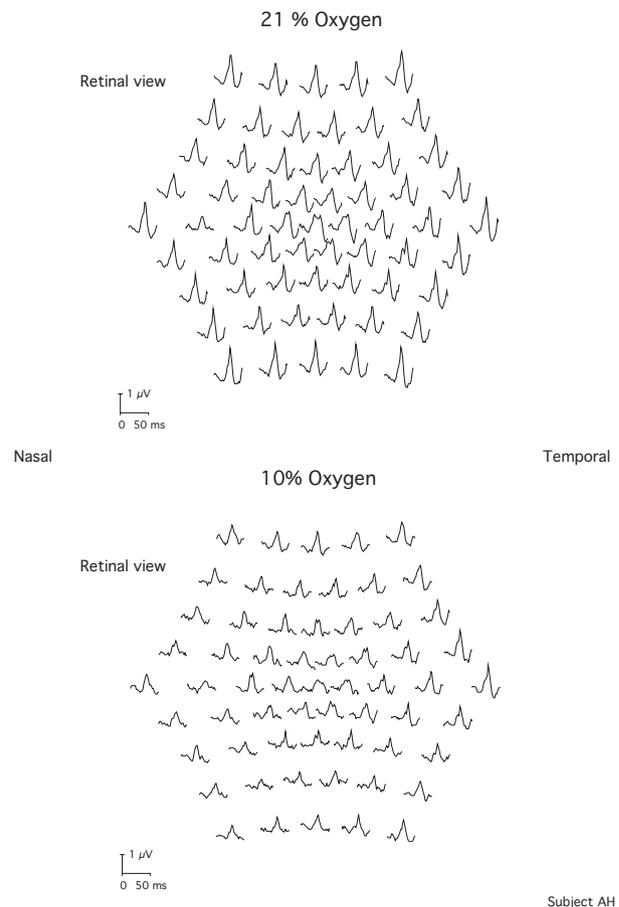Subject AH

FIGURE 3. First-order multifocal ERG responses in a healthy subject breathing atmospheric air (21% oxygen; *top trace array*) and 10% oxygen (*bottom trace array*). The hypoxic recording was made 5 minutes after the switch to 10% oxygen and achievement of a stable P_{O_2}. Hypoxia was associated with an overall mfERG amplitude reduction that decayed with increasing eccentricity.
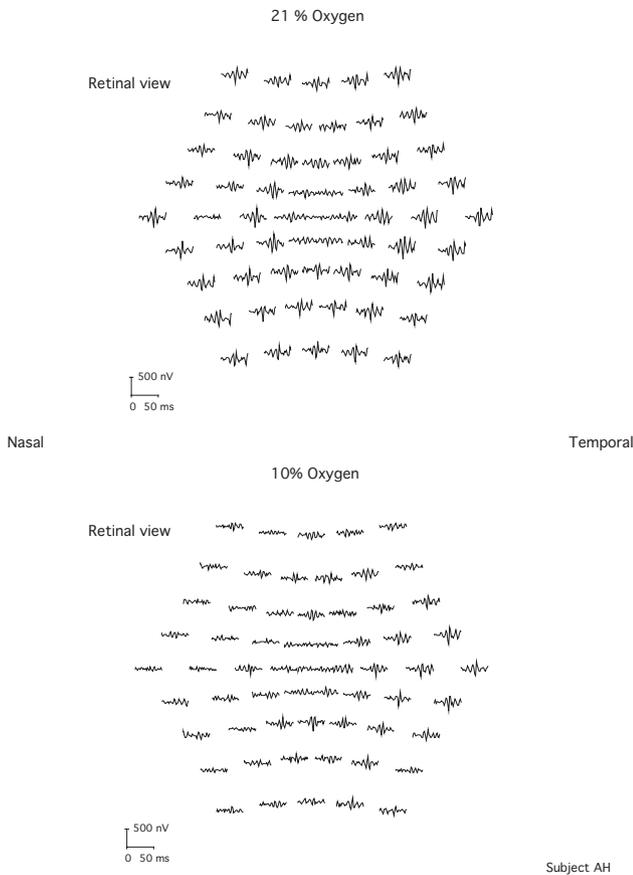
FIGURE 4. Multifocal oscillatory potentials in a healthy subject breathing atmospheric air (21% oxygen; *top trace array*) and 10% oxygen (*bottom trace array*). The hypoxic recording was made 5 minutes after the switch to 10% oxygen and achievement of a stable Po_2. Hypoxia was associated with an overall mfOP amplitude reduction.

sponses. The mean N2 amplitudes from ring 1, 2, and 3 decreased by 28.9% ($P < 0.001$), 28.6% ($P = 0.002$), and 14.9% ($P = 0.021$), respectively, whereas responses averaged from

the two most peripheral rings was unaffected by hypoxia. The second-order N1 and P1 amplitudes and N1, P1, and N2 implicit times were not significantly affected by hypoxia (data not shown).

Hypoxia significantly reduced mean amplitudes of the mfERG oscillatory potentials (OP1 and OP2). As for the primary mfERG responses, the effect was larger for the central responses, reducing amplitudes by 33.8% and 34.8%, respectively (Table 2). This reduction was significant for all rings. The sensitivity of the OP to hypoxia varied less with eccentricity than did the primary mfERG responses. Hypoxia induced a delay of 0.44 ms in the summed OP1 implicit time (95% CI 0.2–0.7; $P = 0.005$).

Hyperoxia-Induced Changes in the mfERG

Inhalation of 100% oxygen was associated with a tendency to a modest increase (4.7%; 3.42 nV/deg^2, $P = 0.05$) in mean first-order P1 amplitude when all 61 stimulus hexagons were averaged (Table 3). No detectable variation with eccentricity or quadrant was found. N2 and N1 first-order amplitudes were not significantly affected by hyperoxia (Figs. 6, 7). Implicit times were unchanged by hyperoxia (data not shown). Hyperoxia did not affect the mean OP1 or OP2 amplitudes of the mfERG (Table 3).

DISCUSSION

The present study demonstrates that systemic hypoxia considerably reduces the amplitude of the human photopic electroretinographic response and that this reduction varies significantly in relation to visual field eccentricity ($P < 0.0001$).

Hypoxia reduced the first-order P1 amplitude by 38.5% within the 2 central degrees whereas a smaller reduction, by 17.8%, was observed at higher eccentricities. The average N1 amplitudes was reduced by only 9.5% ($P = 0.016$) during hypoxia. The higher resistance to hypoxia of the N1 response is compatible with its being analogous to the a-wave of the full-field ERG and P1's being analogous to the b-wave.[12] Thus, our findings are in agreement with the effect of hypoxia on the scotopic ERG in cats, where hypoxia at Pao_2 of 20 to 30 mm Hg led to an 8.9% decrease in the a-wave amplitude but a 35%
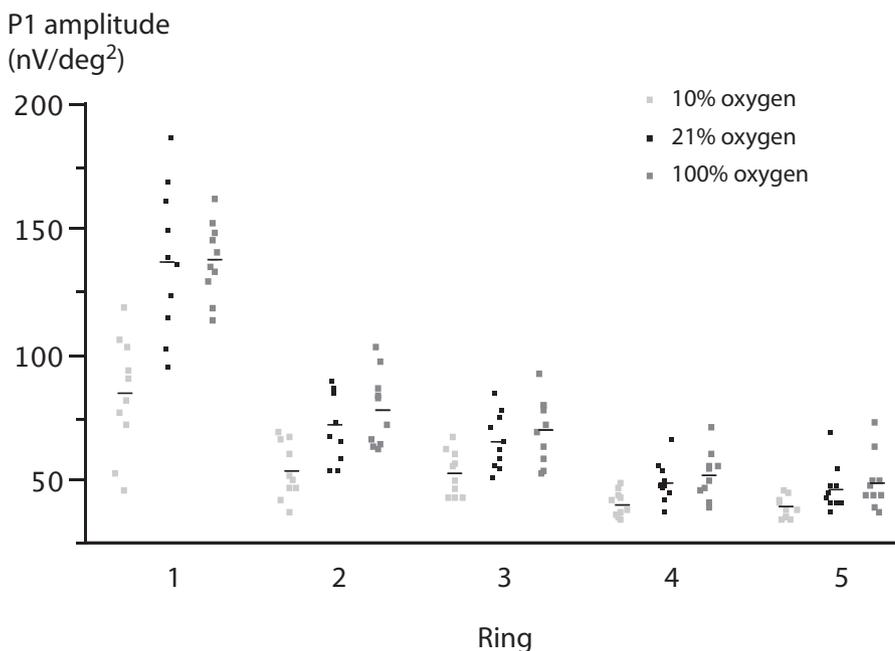
FIGURE 5. The distribution of first-order P1 amplitudes averaged from five rings of increasing eccentricity during hypoxia, normoxia, and hyperoxia. Hypoxia significantly reduced mean P1 amplitudes ($P < 0.0001$). The effect of hypoxia on mean P1 amplitudes decreased with increasing eccentricity ($P < 0.0001$). Hyperoxia increased mean P1 amplitudes modestly, and the effect reached statistical significance only when all 61 stimulated areas were averaged ($P = 0.012$).

TABLE 2. First-Order Amplitudes Averaged from Five Concentric Rings during 10%, 21%, and 100% Oxygen Breathing in Healthy Subjects

Rings	1	2	3	4	5
Amplitudes					
P1					
10%	83.51 ± 24.56	52.51 ± 11.35	51.60 ± 8.66	39.05 ± 5.08	37.52 ± 4.45
21%	135.51 ± 31.15	70.47 ± 14.30	64.10 ± 11.38	47.67 ± 8.00	45.23 ± 9.37
100%	136.71 ± 15.09	76.57 ± 14.89	68.60 ± 12.99	50.52 ± 9.64	47.66 ± 11.07
Difference					
Hypoxia					
P1					
Mean	52.00	17.96	12.50	8.62	7.71
95% CI	(36.8–67.2)	(12.8–23.1)	(7.9–17.1)	(4.16–13.1)	(2.2–13.3)
Δ%	−38.4	−25.48	−19.5	−18.1	−17.1
Hyperoxia					
P1					
Mean	1.20	6.10	4.50	2.85	2.43
95% CI	(−17.5–19.9)	(−1.4–13.6)	(−0.6–9.6)	(−0.7–6.4)	(−1.4–6.3)
Δ%	± 0.9	± 8.7	± 7.0	± 6.0	± 5.4

Rings	1 + 2	3	4	5
Amplitudes				
OP 1				
10%	4.24 ± 1.76	6.53 ± 1.75	3.93 ± 1.05	2.57 ± 0.66
21%	6.40 ± 1.56	7.83 ± 1.80	5.50 ± 1.21	3.85 ± 1.14
100%	6.75 ± 1.64	8.97 ± 2.54	5.43 ± 1.12	4.26 ± 0.87
OP 2				
10%	5.84 ± 1.57	9.88 ± 2.38	7.52 ± 1.37	5.20 ± 0.69
21%	8.96 ± 2.68	13.41 ± 3.35	9.69 ± 1.67	6.82 ± 1.66
100%	8.81 ± 2.69	14.32 ± 3.60	9.82 ± 1.58	7.06 ± 1.83
Difference				
Hypoxia				
OP 1				
Mean	2.16	1.30	1.57	1.28
95% CI	(1.0–3.3)	(0.3–2.3)	(0.6–2.5)	(0.35–2.2)
Δ%	33.8	16.6	28.6	33.3
OP2				
Mean	3.12	3.53	2.17	1.62
95% CI	(1.3–4.9)	(1.9–5.1)	(0.9–3.4)	(0.4–2.9)
Δ%	34.8	26.32	22.4	23.8
Hyperoxia				
OP1				
Mean	0.35	1.14	−0.07	0.41
95% CI	(−1.2–1.9)	(−0.14–2.4)	(−0.8–0.6)	(−0.3–1.1)
Δ%	5.5	14.6	−1.3	10.7
OP2				
Mean	−0.15	0.91	0.13	0.24
95% CI	(−1.9–1.6)	(−0.1–1.9)	(−0.9–1.2)	(−0.5–1.0)
Δ%	−1.7	6.8	1.3	3.5

OP rings 1 and 2 were averaged for better signal to noise ratio. Data are expressed as mean nV/deg^2 ± SD.

decrease in b-wave amplitude.[6] Similar findings have been reported in the human full-field ERG where hypoxia induced by breathing 9% oxygen in 91% nitrogen decreased the scotopic b-wave amplitude by 30%, whereas the a-wave amplitude was unaffected.[13] Thus, the early negative component of the mfERG as well as the full-field ERG seem to be more resistant to hypoxia than the subsequent positive component. Whether this indicates a higher resistance to hypoxia in the outer retina than in the inner retina is uncertain. Thus, it has been shown that only the early phase of the scotopic a-wave response to very bright flashes is generated by direct contribution from photoreceptors and that the postreceptoral activity of OFF pathway cells make a substantial contribution to the a-wave.[14] Likewise, significant contributions to the N1 component of the mfERG have been shown to originate from postreceptor cells in the inner retina.[15] The relatively modest reduction during hypoxia of the second-order mfERG response shown in the present study contradicts the notion of a selective effect of hypoxia on the inner retina.

Inner retinal Po_2 is maintained at a normal level over a wide Pao_2 range, presumably by the autoregulation of the retinal circulation.[16] Nevertheless, retinal Po_2 decreases rapidly below a Pao_2 of 40 mm Hg.[16] In agreement with this, cat[6] and human[13] ERG b-wave amplitudes and—as demonstrated in the present study—the human P1 amplitude, decrease drastically during hypoxia at Pao_2 lower than 40 mm Hg.[16–19] In contrast, milder hypoxia, induced by breathing 12% oxygen in 88% nitrogen, which resulted in levels of PaO_2 higher than 40 mm Hg, was associated with a reduction of only the human photopic b-wave amplitude (by 5.9%).[20]

The electrophysiological changes during hypoxia and hyperoxia reported here are not necessarily direct consequences of isolated changes in Pao_2. Thus, 100% oxygen breathing has been shown to reduce retinal blood flow by 56.4% in healthy subjects.[21] Acidosis induced by hypoxia may also contribute to the mfERG changes shown in our study. Systemic hypoxia in cats has been shown to induce lactacidosis secondary to increased glycolysis,[22] and it has been demonstrated that acidosis
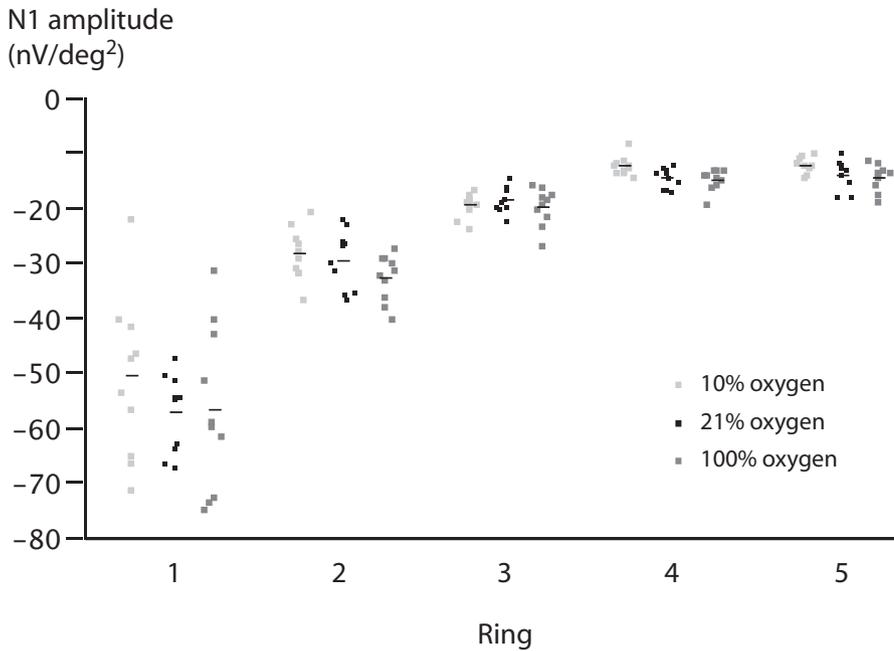
N1 amplitude
(nV/deg^2)

FIGURE 6. The distribution of first-order N2 amplitudes averaged as in Figure 5. Hypoxia significantly reduced mean N2 amplitudes at all eccentricities ($P < 0.01$). As for P1, the effect was most prominent in the central field ($P < 0.001$). N2 first-order amplitudes were not significantly affected by hyperoxia.

reduces the retinal b-wave amplitude.[23] However, only severe hypoxia has been shown to induce acidosis,[24] mainly in the outer retina.[22]

There are only a limited number of reports about variation with eccentricity in the effect of hypoxia on retinal function. Ernest and Krill[25] studied the effect of hypoxia, induced by breathing 10% oxygen in 90% nitrogen, on cone and rod visual thresholds, measured both at 5 and 45° from the fovea. They found rod thresholds at 45° of eccentricity to increase more during hypoxia than did those at 5° of eccentricity. This finding is in contrast to the present study, which demonstrated greater mfERG amplitude sensitivity to hypoxia in the central retina. However, there are obvious limitations in the comparison of the two studies. First, dark adaptometry represents processing of visual inputs in the entire visual system including the brain,

in contrast to the mfERG, which represents retinal responses in isolation. Second, the data in the present study are limited to the central 25° of the retina, in contrast to the more peripheral location (45°) tested by Ernest and Krill. Finally, they demonstrated a higher peripheral sensitivity to hypoxia in rods only, whereas the mfERG responses in this study were cone driven.

A previous study examined the effect of hypoxia on flicker sensitivity at different retinal locations.[26] Hypoxia induced by breathing 5% oxygen in 95% nitrogen was shown to decrease the mean critical flicker frequency (CFF) to values below the normal range. The decrease in CFF was slightly more pronounced in the temporal than in the nasal field, but no significant variation with eccentricity was reported. Thus, flicker sensitivity to hypoxia does not seem to agree with the higher
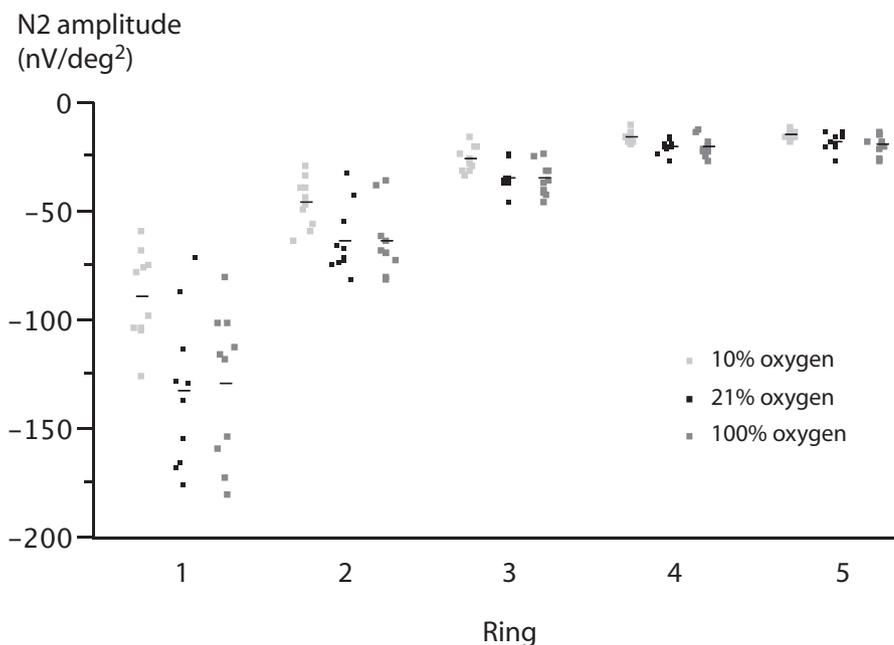
N2 amplitude
(nV/deg^2)

FIGURE 7. The distribution of first-order N1 amplitudes averaged as in Figure 5. As for P1 and N2, mean N1 amplitudes were reduced during hypoxia, but to a lesser extent, and did not reach statistical significance in all rings. The N1 response averaged from all 61 stimulated areas decreased by 9.5% ($P = 0.016$). N1 first-order amplitudes were not significantly affected by hyperoxia.

TABLE 3. Mean Amplitude Differences during Hypoxia, Hyperoxia, and Normoxia Estimated by Mixed-Model Analysis

	P1	OP1	OP2
Hypoxia			
Mean amplitude difference (nV/deg^2)	19.76	1.58	2.61
95% CI	(14.62–24.90)	(0.62–2.50)	(1.23–3.60)
Probability	<0.0001	<0.0001	<0.0001
Variation with ring			
Probability	<0.0001	NS	0.046
Variation with quadrant			
Probability	NS	NS	NS
Hyperoxia			
Mean amplitude difference (nV/deg^2)	3.42	0.46	0.28
95% CI	(0.05–6.88)	(−0.10–1.50)	(−0.23–1.20)
Probability	0.05	NS	NS
Variation with ring			
Probability	NS	NS	NS
Variation with quadrant			
Probability	NS	NS	NS

central mfERG sensitivity shown in this study. However, the authors used a significantly lower spatial resolution and more severe hypoxia than we used in the present study.

A possible explanation of the hypoxia sensitivity reduction with increasing eccentricity in the present study is that the structure and function of the healthy retina vary with eccentricity. First, the fovea is populated entirely by cones, the density of which is higher than elsewhere.[27] However, the metabolic differences between rods and cones are currently unknown and the structure and mitochondrial content of foveal and parafoveal cones are quite different.[28] Although there are fewer parafoveal cones, they are in an environment where rods are using a great deal of energy, at least under dark-adapted conditions. It is also unknown whether rods or cones are better at using glycolytic compensation during hypoxia.

Although the fovea is thinner than the surrounding retina, it is also devoid of retinal vessels in the central 0° to 1.8° (500 μm diameter).[29] There are, however, no inner retinal neurons in the fovea, which may compensate for a longer route of diffusion.[30] In addition, the cells generating the P1 component for the foveal mfERG are displaced away from the center of the fovea, to areas of the perifoveal retina that have a rich blood supply.[30]

Finally, the foveal photoreceptor inner segments are farther from the choroidal circulation than elsewhere, because their outer segments are longer than elsewhere, which may explain some of the variation with eccentricity.[28]

In conclusion, with the mfERG, we have demonstrated profound regional variations in the sensitivity of the retina to hypoxia under photopic conditions in healthy subjects, the fovea being by far most sensitive and the amplitude reduction being prominent, while the implicit time is very nearly unchanged.

References

1. Anderson B Jr, Saltzman HA. Retinal oxygen utilization measured by hyperbaric blackout. *Arch Ophthalmol.* 1964;72:792–795.

2. Ames A 3rd. Energy requirements of CNS cells as related to their function and to their vulnerability to ischemia: a commentary based on studies on retina. *Can J Physiol Pharmacol.* 1992; 70(suppl):S158–S164.

3. Linsenmeier RA. Effects of light and darkness on oxygen distribution and consumption in the cat retina. *J Gen Physiol.* 1986;88: 521–542.

4. Linsenmeier RA, Braun RD. Oxygen distribution and consumption in the cat retina during normoxia and hypoxemia. *J Gen Physiol.* 1992;99:177–197.

5. Braun RD, Linsenmeier RA, Goldstick TK. Oxygen consumption in the inner and outer retina of the cat. *Invest Ophthalmol Vis Sci.* 1995;36:542–554.

6. Kang Derwent J, Linsenmeier RA. Effects of hypoxemia on the a- and b-waves of the electroretinogram in the cat retina. *Invest Ophthalmol Vis Sci.* 2000;41:3634–3642.

7. Arden GB. The absence of diabetic retinopathy in patients with retinitis pigmentosa: implications for pathophysiology and possible treatment. *Br J Ophthalmol.* 2001;85:366–370.

8. Wu S, Sutter EE. A topographic study of oscillatory potentials in man. *Vis Neurosci.* 1995;12:1013–1025.

9. Sutter EE, Bearse MA Jr. The optic nerve head component of the human ERG. *Vision Res.* 1999;39:419–436.

10. Littell RC, Milliken GA, Stroup WW, et al. *SAS System for Mixed Models.* Cary, NC: SAS Institute Inc.; 1996.

11. Severinghaus JW. Simple, accurate equations for human blood O_2 dissociation computations. *J Appl Physiol.* 1979;46:599–602.

12. Hood DC, Seiple W, Holopigian K, et al. A comparison of the components of the multifocal and full-field ERGs. *Vis Neurosci.* 1997;14:533–544.

13. Brown JL, Hill JH, Burke RE. The effect of hypoxia on the human electroretinogram. *Am J Ophthalmol.* 1957;44:57–67.

14. Bush RA, Sieving PA. A proximal retinal component in the primate photopic ERG a-wave. *Invest Ophthalmol Vis Sci.* 1994;35:635–645.

15. Hood DC, Frishman LJ, Saszik S, et al. Retinal origins of the primate multifocal ERG: implications for the human response. *Invest Ophthalmol Vis Sci.* 2002;43:1673–1685.

16. Enroth-Cugell C, Goldstick TK, Linsenmeier RA. The contrast sensitivity of cat retinal ganglion cells at reduced oxygen tensions. *J Physiol.* 1980;304:59–81.

17. McRipley MA, Ahmed J, Chen EP, et al. Effects of adaptation level and hypoglycemia on function of the cat retina during hypoxemia. *Vis Neurosci.* 1997;14:339–350.

18. Linsenmeier RA. Electrophysiological consequences of retinal hypoxia. *Graefes Arch Clin Exp Ophthalmol.* 1990;228:143–150.

19. Linsenmeier RA, Mines AH, Steinberg RH. Effects of hypoxia and hypercapnia on the light peak and electroretinogram of the cat. *Invest Ophthalmol Vis Sci.* 1983;24:37–46.

20. Tinjust D, Kergoat H, Lovasik JV. Neuroretinal function during mild systemic hypoxia. *Aviat Space Environ Med.* 2002;73:1189–1194.

21. Pakola SJ, Grunwald JE. Effects of oxygen and carbon dioxide on human retinal circulation. *Invest Ophthalmol Vis Sci.* 1993;34: 2866–2870.

22. Padnick-Silver L, Linsenmeier RA. Effect of hypoxemia and hyperglycemia on pH in the intact cat retina. *Arch Ophthalmol.* 2005;123:1684–1690.

23. Dawis S, Hofmann H, Niemeyer G. The electroretinogram, standing potential, and light peak of the perfused cat eye during acid-base changes. *Vision Res.* 1985;25:1163–1177.

24. Adams CK, Dawson WW, Perez JM, et al. *Respiratory Stress, Visual Function and Moderation by Chemotherapy. Final Report.* Washington DC: U.S. Army Research and Development Command; 1977.

25. Ernest JT, Krill AE. The effect of hypoxia on visual function: psychophysical studies. *Invest Ophthalmol.* 1971;10:323–328.

26. Wolf E, Nadroski AS. Extent of the visual field: changes with age and oxygen tension. *Arch Ophthalmol.* 1971;86:637–642.

27. Curcio CA, Sloan KR, Kalina RE, et al. Human photoreceptor topography. *J Comp Neurol.* 1990;292:497–523.

28. Hoang QV, Linsenmeier RA, Chung CK, et al. Photoreceptor inner segments in monkey and human retina: mitochondrial density, optics, and regional variation. *Vis Neurosci.* 2002;19:395–407.

29. Anderson B Jr, McIntosh HD. Retinal circulation. *Annu Rev Med.* 1967;18:15–26.

30. Forrester JV, Dick AD, McMenamin G, Lee WR. *The Eye: Basic Sciences in Practice.* 2002:38–39.